AMERICAN SOCIETY FOR MICROBIOLOGY | Antimicrobial Agents and Chemotherapy®

MECHANISMS OF ACTION: PHYSIOLOGICAL EFFECTS

Pyrrolomycins Are Potent Natural Protonophores

Katherine Valderrama,[a] Elizabeth Pradel,[a,e] Alexander M. Firsov,[b] Hervé Drobecq,[a] Hélène Bauderlique-le Roy,[c] Baptiste Villemagne,[d] Yuri N. Antonenko,[b] Ruben Christiaan Hartkoorn[a]

[a]Centre for Infection and Immunity of Lille, U1019-UMR8204, Université Lille, CNRS, INSERM, CHU Lille, Institut Pasteur de Lille, Lille, France
[b]Belozersky Institute of Physico-Chemical Biology, Lomonosov Moscow State University, Moscow, Russia
[c]Flow Core Facility, BioImaging Center of Lille, Institut Pasteur de Lille, Lille, France
[d]Drugs and Molecules for Living Systems, Université Lille, Inserm U1177, Institut Pasteur de Lille, Lille, France
[e]Inserm U995–LIRIC-Lille Inflammation Research International Center, Université Lille, CHU Lille, Lille, France

ABSTRACT The escalating burden of antibiotic drug resistance necessitates research into novel classes of antibiotics and their mechanism of action. Pyrrolomycins are a family of potent natural product antibiotics with nanomolar activity against Gram-positive bacteria, yet with an elusive mechanism of action. In this work, we dissect the apparent Gram-positive specific activity of pyrrolomycins and show that Gram-negative bacteria are equally sensitive to pyrrolomycins when drug efflux transporters are removed and that albumin in medium plays a large role in pyrrolomycin activity. The selection of resistant mutants allowed for the characterization and validation of a number of mechanisms of resistance to pyrrolomycins in both *Staphylococcus aureus* and an *Escherichia coli* Δ*tolC* mutant, all of which appear to affect compound penetration rather than being target associated. Imaging of the impact of pyrrolomycin on the *E. coli* Δ*tolC* mutant using scanning electron microscopy showed blebbing of the bacterial cell wall often at the site of bacterial division. Using potentiometric probes and an electrophysiological technique with an artificial bilayer lipid membrane, it was demonstrated that pyrrolomycins C and D are very potent membrane-depolarizing agents, an order of magnitude more active than conventional carbonyl cyanide *m*-chlorophenylhydrazone (CCCP), specifically disturbing the proton gradient and uncoupling oxidative phosphorylation via protonophoric action. This work clearly unveils the until-now-elusive mechanism of action of pyrrolomycins and explains their antibiotic activity as well as mechanisms of innate and acquired drug resistance in bacteria.

KEYWORDS antibiotic, antibiotic resistance, mechanisms of action, protonophore, pyrrolomycin, uncoupler

Recent reports have brought to light the increasingly devastating emergence of multidrug-resistant pathogenic bacteria (1). To combat this global health care challenge, it is essential that innovative approaches are used to identify novel classes of antibiotics that act through novel vulnerable targets and that are effective against drug-resistant isolates. To date, natural products and derivatives still account for 62% of all approved drugs and for about 80% of approved antibacterial drugs in the period between 1981 and 2014 (2). Nonetheless, due to various factors, including toxicity, poor pharmacokinetics, and lack of *in vivo* efficacy, a multitude of undeveloped natural products with potent *in vitro* antibiotic activity have not been further investigated. Understanding the mechanism of action of such compounds could help evaluate their drug-like potential and uncover novel bacterial targets that are chemically vulnerable. To this extent, in this study, we sought to discover the mechanism of antibiotic activity of pyrrolomycins.

Pyrrolomycins are a group of heavily halogenated small natural antibiotics produced

Citation Valderrama K, Pradel E, Firsov AM, Drobecq H, Bauderlique-le Roy H, Villemagne B, Antonenko YN, Hartkoorn RC. 2019. Pyrrolomycins are potent natural protonophores. Antimicrob Agents Chemother 63:e01450-19. https://doi.org/10.1128/AAC.01450-19.

Address correspondence to Ruben Christiaan Hartkoorn, ruben.hartkoorn@inserm.fr.

Received 18 July 2019
Accepted 31 July 2019
Accepted manuscript posted online 12 August 2019
Published 23 September 2019

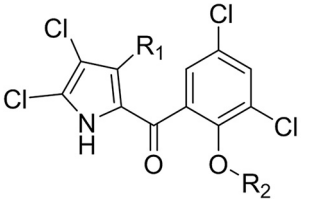

Pyrrolomycin	R_1	R_2
C	H	H
D	Cl	H
I	H	CH_3
J	Cl	CH_3

FIG 1 Chemical structures of pyrrolomycins C, D, I, and J.

by *Streptomyces vitaminophilus* (3), *Streptomyces* sp. strain UC 11065 (4), and *Streptomyces fumanus* (5). Pyrrolomycins carrying a carbonyl linker between the benzyl and pyrrole moiety are reported as potent anti-Gram-positive specific inhibitors (3, 6). Of the many natural pyrrolomycin analogues reported, the pentachlorinated pyrrolomycin D has been shown to be the most potent, with an antistaphylococcal MIC reported at around 1 ng/ml, and activity against biofilms (6), though the minimal bactericidal concentration (MBC) was reported in the low micrograms-per-milliliter range (7). Pyrrolomycin D cytotoxicity has been published to be moderate (6, 8), though its acute toxicity in mice is reported at 20 mg/kg of body weight (following intraperitoneal administration) (3).

The potent activity of pyrrolomycin D could help uncover an innate vulnerability of staphylococci and allow for further chemical optimization of this antibiotic scaffold. In this study, we present illuminating insight into the pyrrolomycin D spectrum of activity, describe diverse mechanisms of bacterial resistance to pyrrolomycins, and define the precise mechanism of action of these natural products.

RESULTS

Chemical synthesis of pyrrolomycins C, D, I, and J. Pyrrolomycins C, D, I, and J (Fig. 1) were successfully produced by *de novo* chemical synthesis and their structures verified by nuclear magnetic resonance (NMR) (see supplemental Results) and high-resolution mass spectrometry. Each of the compounds was found to be more than 95% pure by high-performance liquid chromatography-UV (HPLC-UV) analysis.

***In vitro* profiling of pyrrolomycin activity.** The preferential antibacterial activities of pyrrolomycins C and D against Gram-positive bacteria versus Gram-negative bacteria were confirmed, as previously published (3) (Table 1). Antibiotic susceptibility testing in standard medium (cation-adjusted Mueller-Hinton broth [CAMHB]) confirmed that both *Staphylococcus aureus* and *Streptococcus pneumoniae* were very sensitive to pyrrolomycin D, slightly less sensitive to pyrrolomycin C, and more than 10-fold less susceptible to the methoxy analogues pyrrolomycins I and J (Table 1). The Gram-negative bacteria tested (all cultured in CAMHB) were all an order of magnitude less sensitive to pyrrolomycins than were the Gram-positive bacteria, though pyrrolomycins C and D remained more active than pyrrolomycins I and J (Table 1). *Mycobacterium tuberculosis* (grown in Middlebrook 7H9 supplemented with 10% oleic acid-albumin-dextrose-catalase [OADC], 0.2% glycerol, and 0.05% Tween 80) was weakly susceptible to pyrrolomycins, with similar high MICs for all analogues (Table 1).

To assess whether Gram-negative bacteria were resistant to pyrrolomycins due to their efficient xenobiotic efflux systems, *Escherichia coli* strains lacking a component of the tripartite AcrAB-TolC efflux pump (*E. coli* Δ*tolC*, *E. coli* Δ*acrA,* and *E. coli* Δ*acrB* mutants) were tested for their susceptibility to pyrrolomycins. The data (Table 1) clearly showed that the *E. coli* Δ*tolC* mutant strain is highly sensitive to pyrrolomycins C and D, while surprisingly, the *E. coli* Δ*acrA* and *E. coli* Δ*acrB* mutant strains remained resistant. This suggests that wild-type *E. coli* resistance to pyrrolomycins is due to TolC-mediated efflux (AcrA/B independent) and not due to the absence of a pyrrolomycin intracellular target. The abundance of efficient xenobiotic efflux systems in the other Gram-negative bacteria may also account for their insensitivity to pyrrolomycins.

To investigate the observed insensitivity of *M. tuberculosis* to pyrrolomycins, experiments were designed to evaluate the role of growth medium components. Albumin (as

TABLE 1 MICs and cell line cytotoxicity of pyrrolomycins C, D, I, and J on a panel of bacteria in indicated growth medium[a]

Strain	Culture medium[b]	MIC_{95} (μg/ml) or IC_{95} (IC_{50}) for:					
		Pyr D	Pyr C	Pyr J	Pyr I	Rif	Cipr
S. aureus SH1000	CAMHB	0.025	0.1	1.5	3	0.05	1
S. pneumoniae	CAMHB	0.006	0.1	0.4	3	0.05	1
A. baumannii	CAMHB	3	6.25	>50	>50	>0.2	0.2
K. pneumoniae	CAMHB	5	27	>50	>50	>0.2	0.03
P. aeruginosa PAO1	CAMHB	12.5	33	>50	>50	>0.2	0.125
E. coli BW25113	CAMHB	3	6	>50	>50	>0.2	0.015
E. coli BW25113 Δ*tolC*	CAMHB	0.025	0.0125	1	1.5	>0.2	<0.015
E. coli BW25113 Δ*acrA*	CAMHB	3	/	/	/	/	<0.015
E. coli BW25113 Δ*acrB*	CAMHB	3	/	/	/	/	<0.015
M. tuberculosis H37Rv	7H9-GT-OADC	3	3	4	6	0.005	0.5
S. aureus SH1000	CAMHB + BSA	25	12.5	>50	>50	0.05	1
S. aureus SH1000	CAMHB + FCS	21	21	>50	>50	0.05	1
E. coli BW25113 Δ*tolC*	CAMHB + BSA	33	6	50	25	>0.2	0.015
E. coli BW25113 Δ*tolC*	CAMHB + FCS	12.5	1.5	25	17	>0.2	<0.015
M. tuberculosis H37Rv	7H9-GTy-ND	0.2	0.13	0.83	0.4	0.02	0.25
M. tuberculosis H37Rv	7H9-GTy-ND + BSA	3	1.5	25	25	0.1	0.5
HepG2 (IC_{95} [IC_{50}])	DMEM + FCS	3 (1.1)	1.5 (0.62)	25 (8.3)	29 (8.6)		
HEK-293	DMEM + FCS	3 (1.00)	3 (1.01)	25 (8.52)	25 (7.19)		

[a]Data represent the average of at least 3 replicates. Rifampin (Rif) and ciprofloxacin (Cipr) were used as antimicrobial controls. Pyr, pyrrolomycin; IC_{95}, 95% inhibitory concentration; IC_{50}, 50% inhibitory concentration. Slash indicates that test was not performed.

[b]CAMHB, cation-adjusted Mueller-Hinton broth; CAMHB + BSA, CAMHB supplemented with 0.5% (wt/vol) BSA fraction V; CAMHB + FCS, CAMHB supplemented with 10% (vol/vol) fetal calf serum; 7H9-GT-OADC, Middlebrook 7H9 medium supplemented with 0.2% glycerol, 0.05% Tween 80, and 10% OADC (final concentrations, 0.005% oleic acid, 0.5% albumin fraction V, 0.2% dextrose, 4 mg/liter catalase, and 0.95 g/liter NaCl); 7H9-GTy-ND, Middlebrook 7H9 medium supplemented with 0.2% glycerol, 0.025% tyloxapol, 0.2% dextrose, and 0.95 g/liter NaCl; 7H9-GTy-ND + BSA, Middlebrook 7H9 medium supplemented with 0.2% glycerol, 0.025% tyloxapol, 0.2% dextrose, 0.95 g/liter NaCl, and 0.5% albumin fraction V; DMEM + FCS, Dulbecco's modified Eagle medium supplemented with 10% (vol/vol) fetal calf serum.

bovine serum albumin [BSA]) is traditionally present in the culture medium of *M. tuberculosis* as part of the OADC or ADC supplements and functions to prevent toxicity associated with the Tween 80 detergent (9). However, albumin is known to bind drugs/compounds and alter their free fraction in medium, potentially affecting activity. Indeed, by using a medium supplemented with tyloxapol instead of Tween 80, it was clearly demonstrated that the removal of BSA rendered *M. tuberculosis* 10 times more susceptible to pyrrolomycins (Table 1). In a reverse experiment, the addition of BSA or fetal calf serum (FCS) to CAMHB reduced the activity of pyrrolomycin against *S. aureus* and the *E. coli* Δ*tolC* mutant by at least 2 orders of magnitude (Table 1). Overall, these data clearly suggest that pyrrolomycins are highly bound to albumin, and that differences in culture medium composition, particularly the presence of albumin, help explain the previously described low sensitivity of *M. tuberculosis* to pyrrolomycins.

The impact of medium supplementation with BSA or FCS (typically used in cell culture medium) also calls into question the validity of the previously reported high selectivity index (antibiotic activity versus cytotoxic activity) of pyrrolomycins (6, 8). Interestingly, the cytotoxicity of pyrrolomycins observed here against HepG2 and HEK293 human cells was in the same range as that observed for Gram-positive bacteria grown with 10% FCS supplementation (Table 1). These data illustrate that when correcting for differences in medium composition, there is no selectivity of pyrrolomycins C, D, I, or J for bacterial versus eukaryotic cells. This finding may explain the reported acute toxicity of pyrrolomycins in mice of 50 and 20 mg/kg for pyrrolomycins C and D, respectively (3).

Time-dependent killing and MBC. Previous published data showed a large difference between the MIC and the minimal bactericidal concentration (MBC) for pyrrolomycins (7). This result was confirmed here, and the data show that the bactericidal activity is both concentration and time dependent (Fig. S1). Following a 24-h pyrrolomycin D exposure, a 2-log drop in CFU was achieved against *S. aureus* SH1000 and the *E. coli* Δ*tolC* mutant at 3 μg/ml and 0.75 μg/ml, respectively, compared to an MIC of 25 ng/ml for both strains. Analysis of the time-dependent bactericidal activity at 200 ng/ml (8 times MIC) showed a slow but gradual decline in CFU for both *S. aureus* SH1000 and the *E. coli* Δ*tolC* mutant (Fig. S1).

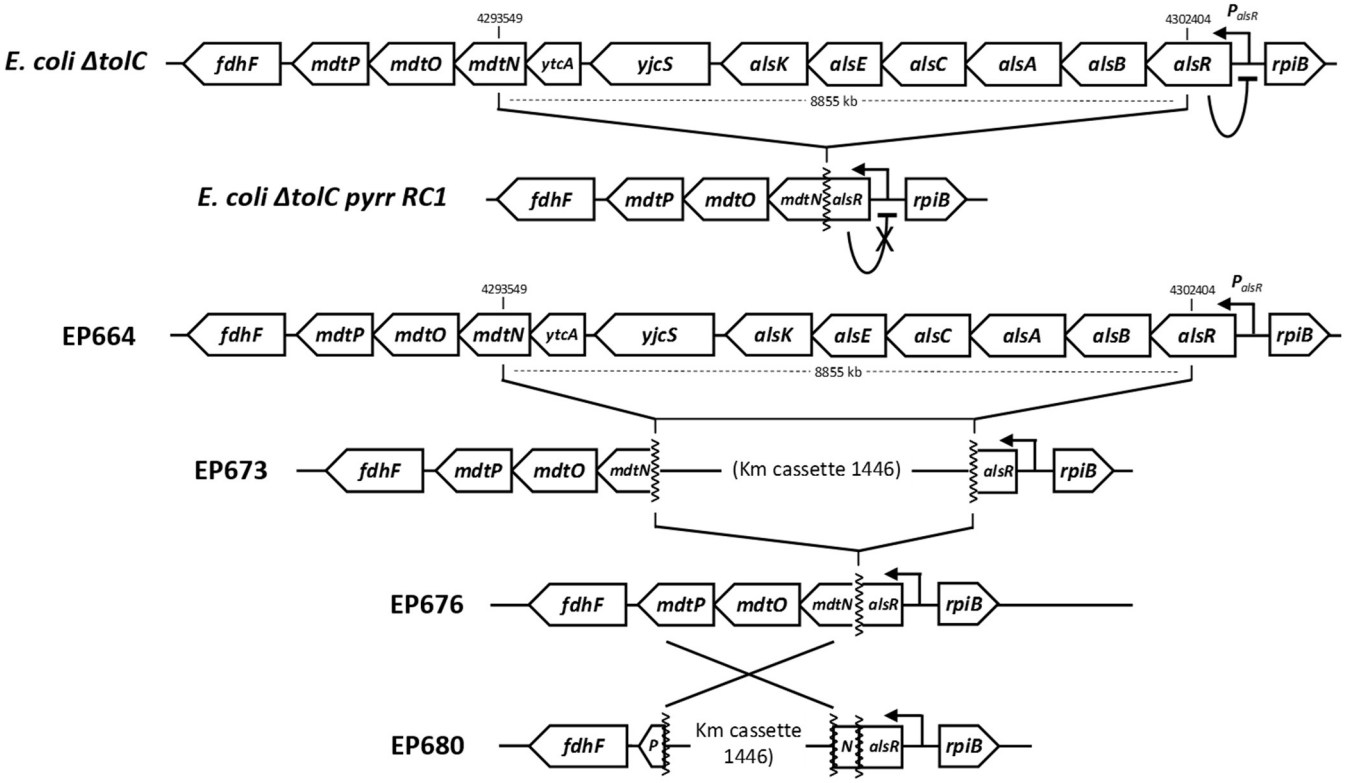

FIG 2 Illustration of the genetic arrangement found in pyrrolomycin-resistant *E. coli* isolates, and engineered validation strains. From the parental *E. coli* Δ*tolC*::Km strain, a pyrrolomycin D-resistant isolate, *E. coli* Δ*tolC pyrr RC1,* was sequenced and shown to bear a 8,855-bp deletion between bases 4293549 and 4302404, deleting 7 whole genes and 2 partial genes, and forming a hybrid in-frame gene between the truncated *alsR*′ and ′*mdtN* genes. The disruption of the *alsR* gene (encoding a transcriptional repressor) likely leads to derepression of the *als* promoter P_{als}. Deletion mutants were generated via Red recombineering to validate that resistance was due to *mdtOP* expression via P_{als} derepression. To achieve this, the original *E. coli* Δ*tolC*::Km mutant strain was deleted of its Km cassette to obtain EP664 Δ*tolC*. The 8,855-bp *als* locus was then deleted and replaced with a Km cassette transcribed in the orientation opposite the *als* and *mdt* genes to yield EP673. EP673 was then cured of the Km cassette to generate EP676. Finally, to determine the involvement of *mdtO* and *mdtP*, these genes were deleted and replaced by a Km cassette to obtain EP680.

Deciphering genetic resistance to pyrrolomycin D. (i) Pyrrolomycin D resistance in the *E. coli* Δ*tolC* mutant. To gain an insight into the mechanism of action of pyrrolomycin D, efforts were made to select resistant bacteria from the *E. coli* Δ*tolC* mutant and *S. aureus* streaked grown on solid medium containing pyrrolomycin D at concentrations above its MBC (1 μg/ml). Despite numerous attempts, and the addition of up to 6×10^{10} bacteria per plate (100 μl of optical density at 600 nm [OD_{600}] of 400), no resistant *S. aureus* clone could be isolated. For the *E. coli* Δ*tolC* mutant, when 2×10^{10} CFU were plated, two resistant colonies were isolated. Following culture of the resistant clones in compound-free medium, the resistance to pyrrolomycin D was confirmed (MIC, 2 μg/ml). Whole-genome sequencing and variant analysis of one of the resistant mutants (*E. coli* Δ*tolC pyrr RC1*) revealed no single nucleotide polymorphism, nor short insertion or deletion, but instead a large deletion between positions 4293549 and 4302404 on the genome reference (accession no. CP009273.1). This 8,855-bp deletion, confirmed by Sanger sequencing, encompasses nine genes transcribed in the order *alsR*, *alsB*, *alsA*, *alsC*, *alsE*, *alsK*, *yjcS*, *ytcA*, and *mdtN* (Fig. 2). The second pyrrolomycin-resistant clone that was isolated contained the exact same deletion. The role of this large deletion in pyrrolomycin resistance was confirmed using a genetic engineering approach on *E. coli* strain EP664 (BW25113 Δ*tolC,* where the kanamycin cassette was removed by FLP recombination target [FRT] excision). Replacement of the 8,855-bp region in EP664 with a kanamycin resistance cassette (resulting in *E. coli* strain EP673) was found not to alter its pyrrolomycin D sensitivity (Table 2). However, subsequent erasing of the kanamycin cassette by allelic exchange to generate the unmarked *pyrr RC1* deletion in strain EP676 conferred resistance to pyrrolomycin D

TABLE 2 Resistance profiles of *E. coli* BW25113 Δ*tolC* strains to pyrrolomycins D and C

Strain	Characteristics	MIC_{95} (μg/ml) for:		
		Pyr D	Pyr C	Km
Δ*tolC* mutant	Δ*tolC*::Km	0.025	0.125	>50
Δ*tolC pyrr RC1* mutant	Δ*tolC*::Km, with selected pyrrolomycin resistance	3	6	>50
EP664	Δ*tolC*	0.025	0.125	4
EP673	Δ*tolC* Δ*alsRBACEK-yjcS-ytcA-mdtN*::Km	0.025	0.125	>50
EP676	Δ*tolC* Δ*alsRBACEK-yjcS-ytcA-mdtN*	3	6	4
EP680	Δ*tolC* Δ*alsRBACEK-yjcS-ytcA-mdtNOP*::Km	0.025	0.125	>50
EP676(pEP713)	Empty plasmid bearing PgapA (control)	0.5		
EP676(pEP712)	*PgapA-alsR* plasmid (*alsR* overexpression)	0.062		
EP664(pBAD30)	Empty plasmid without arabinose	0.062		
EP664(pBAD30)	Empty plasmid with 10 mM arabinose	0.062		
EP664(pEP714)	pEP714 is pBAD30::*mdtP*, without arabinose	0.062		
EP664(pEP714)	pEP714 is pBAD30::*mdtP*, with 10 mM arabinose	1		

(Table 2). This work confirmed the causality of the 8,855-bp deletion in pyrrolomycin resistance and showed that resistance was likely due to the new gene arrangement rather than to the gene loss.

The deletion in *E. coli* Δ*tolC pyrr RC1* and EP676 places the *mdtO* and *mdtP* genes in close proximity to the *als* operon promoter (P_{als}). *mdtO* and *mdtP* encode resistance-nodulation-division (RND)-type multidrug efflux pump components homologous to AcrB (inner membrane transporter) and TolC (outer membrane channel), respectively. Thus, we reasoned that the P_{als} promoter activity may be high in EP676, as the local repressor gene *alsR* is truncated due to the deletion, and that *mdtP* overexpression could complement the loss of *tolC*. To verify these hypotheses, several genetic constructs were generated and evaluated. First, when the *mdtOP* genes were deleted in EP676, the resulting strain, EP680, turned pyrrolomycin sensitive, confirming the role of *mdtOP* in pyrrolomycin resistance (Table 2). Second, conditional expression of *mdtP* alone in EP664, a Δ*tolC* mutant strain bearing an intact *als-mdt* locus, led to a pyrrolomycin resistance phenotype, showing that the overproduction of the MdtP outer membrane channel was sufficient for pyrrolomycin resistance (Table 2). Finally, the overexpression of *alsR* from a plasmid rendered EP676 sensitive to pyrrolomycin D (Table 2), confirming the role of the *als* promoter and that of the AlsR repressor. Overall, these results demonstrate that the pyrrolomycin resistance phenotype selected is due to a genetic rearrangement that results in the *als* promoter-mediated upregulation of *mdtP*.

(ii) Selection of pyrrolomycin D-resistant clones from *E. coli* EP680. To isolate alternative pyrrolomycin-resistant *E. coli* mutants devoid of mutations associated with the MdtP channel, 1×10^9 EP680 (Δ*tolC* Δ*als-mdtNOP*) cells were deposited on plates containing low concentrations of pyrrolomycin D (50 ng/ml, twice the solid MIC). Seven colonies appeared after 48 h. All colonies were confirmed to present low-level resistance to pyrrolomycin D (Table 3). Whole-genome sequencing and variant analysis on two selected resistant clones (EP680-RC50.6 and EP680-RC50.11) revealed that both isolates carried a point mutations in *slyA* (encoding a nonessential transcriptional regulator of the MarR family), while the more resistant clone, EP680-RC50.6, carried an additional point mutation in *ompA* (outer membrane protein A) (Table 3). These

TABLE 3 Pyrrolomycin D sensitivity of *E. coli* Δ*tolC* mutant strains on solid medium

E. coli strain	Characteristics	Solid pyrrolomycin D MIC (ng/ml)
EP680	Δ*tolC* Δ*alsRBACEK-yjcS-ytcA-mdtNOP*::*Km*	40
EP680-RC:50.6	*slyA*(Q49H) *ompA*(G63R)	80
EP680-RC:50.11	*slyA*(W16stop)	60
EP664	Δ*tolC*	40
EP705	EP664 Δ*ompA*	30
EP706	EP664 Δ*slyA*	50

TABLE 4 Sensitivity of *S. aureus* SH1000 and isolates resistant to pyrrolomycin D and daptomycin as measured on solid medium

S. aureus strain	SNP identified relative to SH1000[a]	Solid pyrrolomycin D MIC (ng/ml)	Daptomycin MIC_{95} (μg/ml)
SH1000	WT	20	1.25
100-1	*mprF*(L78Stop) (WGS) (S), 1797388(t→g) (WGS) (S)	35	0.078
100-2	*mprF*(L78Stop) (S), 1797388(t→g) (S)	30	0.078
100-3	*mprF*(Y419Stop) (S)	35	0.078

[a]The genetic variations identified by whole-genome sequencing (WGS) or targeted Sanger sequencing (S) are shown. WT, wild type.

mutations were confirmed by Sanger sequencing. The mutations in *slyA* were a premature stop codon at position 16 in one clone and a point mutation at the beginning of the helix-turn-helix (HTH) domain (Q49R) in the other clone, both likely generating a dysfunctional proteins. Pyrrolomycin susceptibility studies of the *E. coli* Δ*tolC* Δ*slyA* mutant (EP706) confirmed that *slyA* inactivation confers low-level pyrrolomycin resistance (Table 3). The role of SlyA in *E. coli* is still poorly known, but it is a MarR-type transcriptional regulator that targets numerous bacterial promoters (10). Though it is not clear how the inactivation of *slyA* causes low-level pyrrolomycin D resistance in *E. coli*, in *Salmonella enterica*, *slyA* (91% identical) has been shown to be involved in resistance to antimicrobial peptides (11). The mutation found in *ompA* (G63R) is located in the second transmembrane β-barrel of the protein. In contrast to this mutation, the deletion of *ompA* in the Δ*tolC* background rendered *E. coli* similarly sensitive (perhaps slightly more sensitive) to pyrrolomycin D, comparable to the susceptibility data reported for other antibiotics (12). While the role of OmpA in antibiotic susceptibility is still debated, it is believed that its role in susceptibility to non-beta-lactam antibiotics is by altering membrane integrity and permeability rather than antibiotic transport (12), with the identified mutations presumably resulting in a gain-of-function phenotype.

(iii) Selection of pyrrolomycin D-resistant clones from *S. aureus* SH1000. As no *S. aureus* resistant mutant could be isolated on high concentrations of pyrrolomycin D, selection was repeated at near MICs. Three resistant colonies could be isolated when 1.5×10^{10} CFU were plated at a concentration of 4 times the MIC (100 ng/ml). As with *E. coli* EP680 resistant mutants, these isolates appeared only after 48 h and were confirmed to have low-level resistance to pyrrolomycins D and C (Table 4). One of these resistant isolates (100-1) and the parental SH1000 *S. aureus* strain were subjected to whole-genome sequencing and variant analysis. The data showed a point mutation in the nonessential *mprF* gene (L78Stop) and a second one in the region upstream of the *SAOHSC_01883* gene (conserved hypothetical), both confirmed by Sanger sequencing. Targeted sequencing of these regions in the two other resistant isolates showed that clone 100-2 carried the same mutations as clone 100-1, and that clone 100-3 carried a single-base insertion in *mprF* resulting in a premature stop codon. As different mutations in *mprF* were found in two resistant isolates, mutations in this gene are likely associated with pyrrolomycin resistance.

mprF codes for a multiple peptide resistance factor (MprF) with phosphatidylglycerol lysyltransferase activity that modifies membrane phosphatidylglycerol (PG) to lysyl-phosphatidylglycerol (LPG). Increased *mprF* expression has been demonstrated to increase the cationic charge of the bacterial membrane and repel cationic molecules, such as daptomycin (13, 14), methicillin (15) (where *mprF* is named *fmtC*), and several other cationic antibacterial peptides (16). Bearing this in mind, the daptomycin susceptibility of the pyrrolomycin D-resistant isolates was determined, and all three were found to be 16-fold more sensitive than was the parental *S. aureus* strain (Table 4). This suggests that the absence of MrpF decreases the cationic charge of the membrane and favors daptomycin entry. As pyrrolomycin D is predicted to be anionic at physiological pH, decreasing the cationic charge of the membrane will likely disfavor its penetration and hence lead to low-level resistance.

Pyrrolomycin D is not an electrophile, and its activity is not impacted by antioxidants. Pyrrolomycin D did not react with glutathione and hence is unlikely an

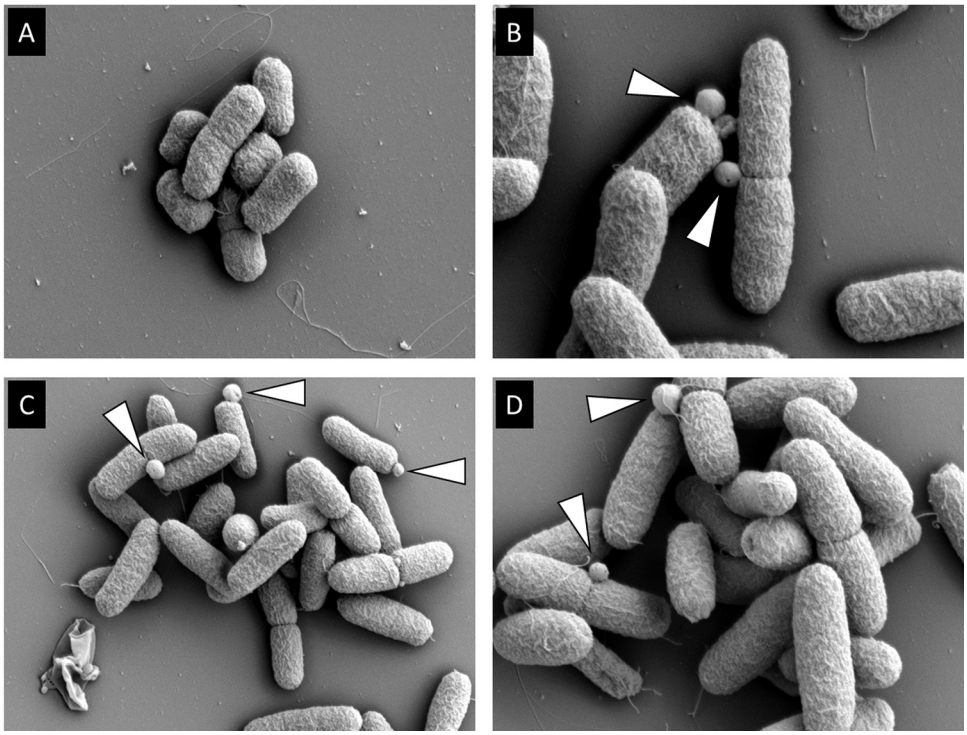

FIG 3 (A to D) SEM images of the *E. coli* Δ*tolC* mutant following a 5-h exposure to DMSO (A) or 100 ng/ml pyrrolomycin D (B to D, three representative SEM images). Cell wall blebs can be clearly observed on pyrrolomycin-exposed bacteria (indicated by white triangles).

electrophile that could target proteins nonspecifically (data not shown). Similarly, pyrrolomycin activity against *S. aureus* was not impacted by antioxidants, such as α-tocopherol or ascorbic acid (data not shown), suggesting that activity was not mediated through reactive radical species. To gain a first insight into whether pyrrolomycins can affect membrane potential, the impact of pH on pyrrolomycin activity was determined. The data clearly show that decreasing the medium pH improved the activity of pyrrolomycin D against both *S. aureus* and the *E. coli* Δ*tolC* mutant, similarly to the effect observed with the proton uncoupler carbonyl cyanide *m*-chlorophenylhydrazone (CCCP) (see Fig. S2 in the supplemental material).

Visualization of pyrrolomycin D activity by SEM. Scanning electron microscopy (SEM) was used to determine potential changes in *E. coli* and *S. aureus* morphology following pyrrolomycin D exposure. Initial observations performed after 5 h exposure of 1 μg/ml pyrrolomycin D showed that most bacteria were no longer intact. To obtain images of cellular deformation prior to bacterial cell wall collapse, lower concentrations of pyrrolomycin D were used (100 ng/ml). With respect to *S. aureus*, no obvious consistent bacterial deformation could be observed following bacterial exposure. In contrast, blebbing or bulging of the *E. coli* Δ*tolC* mutant cell wall was clearly observed in the presence of pyrrolomycin D (Fig. 3). This deformation was largely localized at the division septum, sometimes seen at the old pole, and was reminiscent of images of *E. coli* following exposure to the antimicrobial peptide human defensin 5 (HD5) (17). Altogether, these data suggest that pyrrolomycins act by increasing the bacterial osmotic pressure that leads to local bacterial cell wall rupture and bleb generation, or by weakening the cell wall so that it is no longer able to contain the normal osmotic pressure.

Impact of pyrrolomycin D on *S. aureus* membrane potential. To determine whether pyrrolomycins act as proton gradient-depolarizing agents, the potentiometric probe 3,3′-dipropylthiadicarbocyanine iodide [DiSC3(5)] was initially used. DiSC3(5) accumulates readily in bacteria with polarized membrane, and this strong accumulation

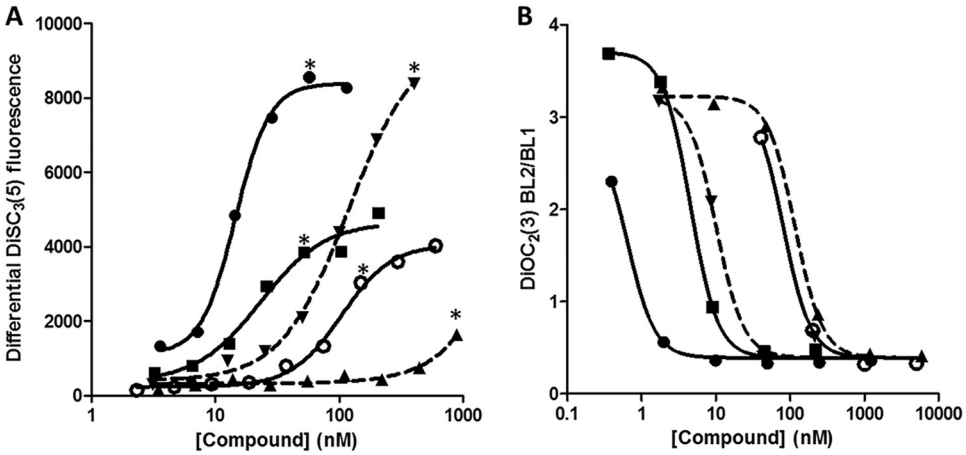

FIG 4 (A and B) *S. aureus* membrane potential measured using potentiometric dyes $DiSC_3(5)$ (A) and $DiOC_2(3)$ (B) in the presence of pyrrolomycin C (filled circle, solid line), D (filled square, solid line), I (filled inverted triangle, dotted line), J (filled triangle, dotted line), and CCCP (open circle, solid line). Asterisks indicate concentrations at which the molecules quench the fluorescence signal of $DiSC_3(5)$.

causes self-quenching of its fluorescence signal. Upon depolarization of the membrane, DiSC3(5) is released, quenching is decreased, and fluorescence is increased. As previously reported (18), we found that in the absence of cells, the proton uncoupler CCCP, but also pyrrolomycins C and D, cause a concentration-dependent quenching of DiSC3(5) (quenching observed above 0.038 and 0.019 μg/ml, respectively). We confirmed that this quenching is not mediated by CCCP or pyrrolomycin absorbance of the DiSC3(5) excitation or emission wavelengths. To our knowledge, the mechanism of this interaction remains unknown. Due to the observed quenching, compound-dependent depolarization of bacterial membranes was evaluated at subquenching concentrations. The data showed that pyrrolomycin C was particularly potent at depolarizing the *S. aureus* membrane, with the methylated pyrrolomycin I being significantly less active. Pyrrolomycin D also caused depolarization at a very low concentration; however, the magnitude of the depolarization [$DiSC_3(5)$ signal change] was inferior to that of pyrrolomycin C but comparable to that of CCCP (Fig. 4). Overall, these data suggest that pyrrolomycins C and D are more potent modulators of the membrane potential of *S. aureus* than CCCP.

To confirm that pyrrolomycins cause membrane depolarization in bacteria, an alternative potentiometric probe, $DiOC_2(3)$, was used in combination with flow cytometry. This assay follows $DiOC_2(3)$ changes in fluorescence from red (BL2) to green (BL1) following membrane depolarization (measured by the BL2/BL1 ratio; Fig. 4). In contrast to $DiSC_3(5)$, we did not observe quenching of $DiOC_2(3)$ upon the addition of pyrrolomycins or CCCP. In agreement with data obtained using $DiSC_3(5)$, we found that pyrrolomycins C and D were nanomolar modulators of membrane potential, with pyrrolomycin C being 1 log more potent than pyrrolomycin D and 2 orders of magnitude more potent than CCCP. The methylated pyrrolomycins I and J were more than 10-fold less potent than their respective analogues pyrrolomycins C and D, but they were still able to depolarize the *S. aureus* membrane potential at higher concentrations (Fig. 4).

Impact on mitochondrial respiration. Mitochondrial respiration (oxygen consumption) is a direct result of the electron transport chain maintaining a resting proton motive force (electrochemical gradient) that drives ATP synthesis through the ATP synthase. The addition of uncoupler depletes the proton motive force and the mitochondria (as well as bacteria) response by increasing proton efflux through an increase in the electron transport chain activity and, hence, respiration. In experiments measuring rat liver mitochondrial respiration, both pyrrolomycins C and D were potent stimulators of respiration, a feature commonly seen following the addition of proto-

nophoric uncouplers (Fig. S3). This potent nanomolar activity on isolated mitochondria is likely associated with pyrrolomycin cytotoxicity to eukaryotic cells.

Protonophore activity of pyrrolomycins D and C on a planer lipid bilayer. To examine the protonophoric activity of pyrrolomycins D and C in a pure lipid membrane system, we measured electric current across a planar lipid bilayer (BLM) under voltage-clamp conditions (Fig. 5A). As seen in Fig. 5B, the addition of nanomolar concentrations of pyrrolomycin D to bathing solutions at both sides of BLM induced a transmembrane electric current in a nanoampere range (voltage, 25 mV), and the value of the current increased with pyrrolomycin D concentration.

To determine the ion selectivity of pyrrolomycin D-mediated permeability, current-voltage (I-V) curves were measured under symmetrical (equal pH in both chambers) and asymmetrical (a different pH in both chambers; pH 1 = 7.0, pH 2 = 8.2) conditions (Fig. 5C). The value of zero-current potential (V_{zero}) under asymmetrical conditions was −57 mV, corresponding to the high proton selectivity of the conductance ($V_{theoretical}$ = RT/F ΔpH = −71 mV at ΔpH = 1.2). As pyrrolomycin D, pyrrolomycin C demonstrated good proton selectivity, with a V_{zero} of −46 mV at ΔpH 1.2.

To place the protonophoric activity of pyrrolomycins in the context of the conventional protonophore CCCP, a comparison was performed at a 3 μM concentration of the compounds. Remarkably, pyrrolomycin D demonstrated much greater protonophoric activity (BLM current) than did the uncoupler CCCP (Fig. 5C). The activity of pyrrolomycin C was lower than that of pyrrolomycin D but still superior to that of CCCP (Fig. 5D). The larger protonophoric activity of pyrrolomycin D compared to pyrrolomycin C can be tentatively ascribed to better permeability of the compound with five chloride atoms (pyrrolomycin D) than with four chloride atoms (pyrrolomycin C). It has been shown earlier that chlorination increased the membrane permeability of hydrophobic anions (19, 20).

DISCUSSION

Thanks to their many functions, natural products are an incredibly rich source of antibiotic or antifungal molecules but also of potent anticancer agents and immunomodulatory molecules. Pyrrolomycins, produced by *Streptomyces vitaminophilus* and other bacteria, are described as some of the most potent natural antibiotics known, with activities in the low-nanomolar range against Gram-positive bacteria (3), as well as activity against biofilms (6). Other natural products share a similar chemical scaffold, such as pyoluleorin (21), TAN-876B (22), and marinopyrroles (23). Interestingly, while all these molecules are described as antibiotics, their mechanisms of actions are still elusive. By investigating the mechanism of action of pyrrolomycins, this work highlights the antibiotic drug potential of pyrrolomycins.

An important finding is that the antibiotic activity of pyrrolomycins is not specific to a select number of Gram-positive bacteria, as previously reported, but is instead much more general. We clearly demonstrated that *E. coli*, and probably other Gram-negative bacteria, are resistant to pyrrolomycins due to efflux of the xenobiotic through a TolC-dependent AcrAB-independent efflux system rather than to the absence of a target. In addition, our studies demonstrated that *M. tuberculosis* insensitivity to pyrrolomycins is due to the presence of BSA in the growth medium, which likely binds pyrrolomycins and sequestrates it away from the bacteria. The impact of both BSA and FCS in growth medium calls into consideration the previously reported high selectivity window of pyrrolomycins over eukaryotic cells in cytotoxicity assays, which contrasted with its reported acute toxicity in mice (3). These data show that one must be very careful when evaluating the spectrum of activity of antibacterial compounds, taking great care to account for differences caused by environmental factors such as growth medium.

Investigating the mechanism of resistance to a compound can often help clarify its mode of action. For most known antibiotics that target essential enzymes or the ribosome, there is an attainable frequency of resistance with mutations appearing in the target (rifamycins, beta-lactam antibiotics, fluoroquinolones, and aminoglycosides). However, when compounds act on nongenome-encoded targets, such as membrane

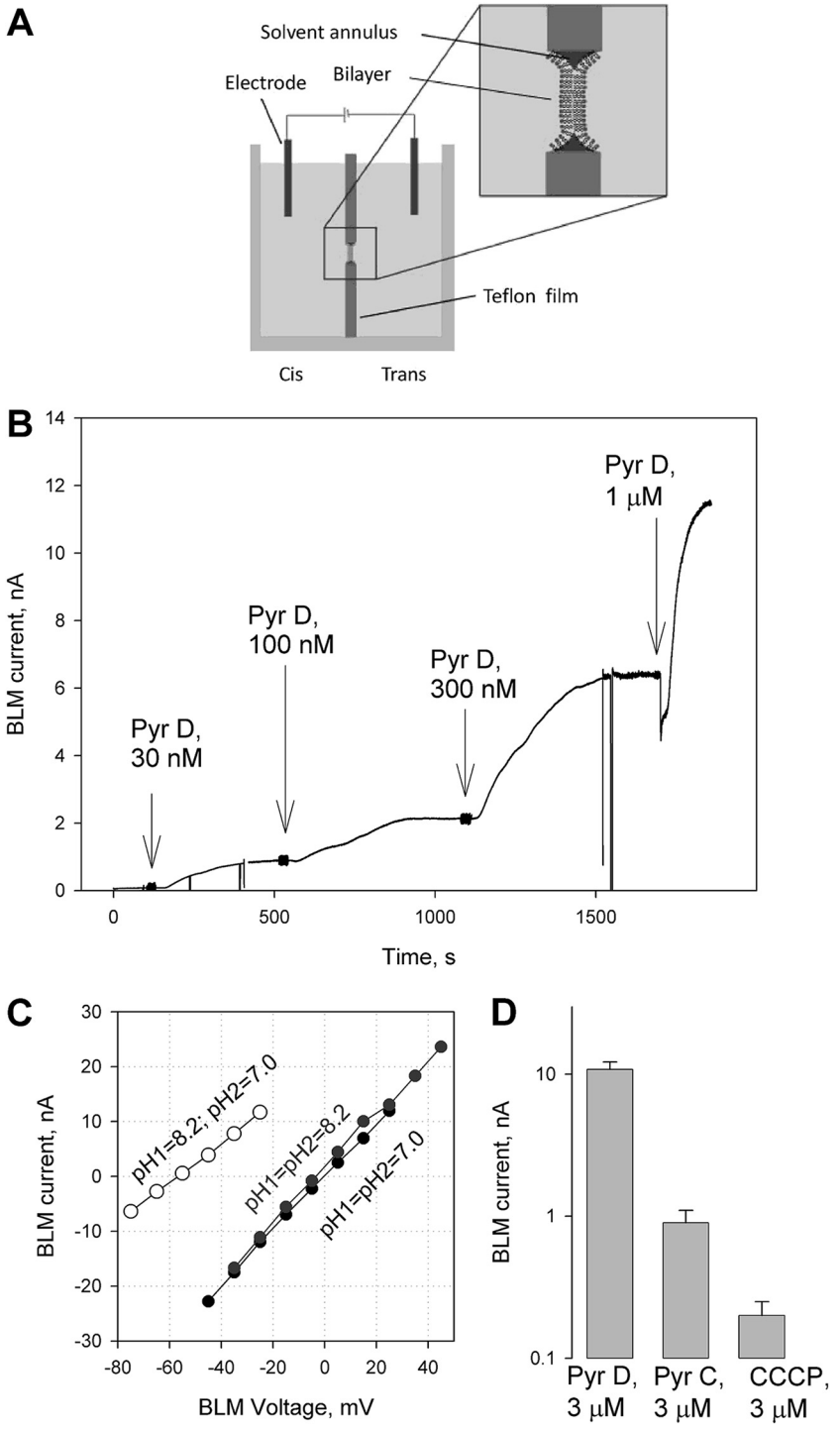

FIG 5 (A). A schematic of the BLM (made from DPhPC) electrophysiological setup used to determine the protonophoric activity of pyrrolomycin. (B) Induced electrical current through planar BLM following the addition of indicated concentrations of pyrrolomycin D to both the *cis* and *trans* chambers. The solution was 50 mM Tris, 50 mM MES, and 10 mM KCl (pH 7.0). The BLM voltage was 25 mV. (C) Current-voltage (I-V) curves for 1 μM pyrrolomycin D under symmetrical (both *cis* and *trans* chambers at pH 7.0, black line, or both at pH 8.2, red line) and asymmetrical conditions (*cis* chamber at pH 7.0, *trans* chamber at pH 8.2, blue line). (D) Electrical current (in nanoamperes) induced through DPhPC membrane by 3 μM pyrrolomycin D, pyrrolomycin C, and CCCP (mean $\pm$ standard deviation [SD]; $n = 4$).

lipids, sugars, or peptidoglycans, as is the case for vancomycin, teixobactin (24), or daptomycin (25), the frequency of resistance is often very low, with mutations associated with proteins involved in compound penetration or in the formation of nongenome-encoded targets. The difficulty of obtaining target-associated mutations is suggestive of a nonprotein, nonribosomal target. The few pyrrolomycin-resistant mutants that could be isolated in this work showed low-level resistance, and the mutation most probably affects compound penetration by affecting membrane charge. The only mutation found to cause higher-level resistance was identified in the *E. coli* Δ*tolC* mutant and was due to a large genomic deletion that placed the *mdtOP* efflux genes under the control of a now-active promoter (due to the loss of the AlsR transcriptional repressor). Genetic validation experiments clearly identified that overproduction of the MdtP outer membrane channel is able to phenocopy pyrrolomycin resistance through a mechanism that remains to be defined, but it likely equates to pyrrolomycin efflux from the bacteria, although it is AcrAB independent.

A combination of techniques (scanning electron microscopy, pH-mediated changes in MIC, and potentiometric dyes) were used to help narrow down the likely mode of action of pyrrolomycins to the perturbation of the bacterial membrane potential. Nevertheless, membrane potential can be perturbed by multiple mechanisms, direct or indirect (pore-forming toxins, the perturbation of ion channels, ion pumps, ionophores, etc.). To this extent, the BLM experiments were crucial to demonstrate that pyrrolomycins can specifically move protons across a BLM (containing no protein) in a dose-dependent manner. This clearly defined the mechanism of action of pyrrolomycins to be protonophores capable of depolarizing bacterial membranes and uncouple their oxidative phosphorylation. An efficient proton uncoupler needs to remain associated with the membrane and to have an ionizable group to allow for the transfer of protons from outside the membrane to the cytoplasm. Both pyrrolomycins C and D are very lipophilic (predicted logP values, 4.91 and 5.51, respectively, MarvinSketch 18.23.0; Chemaxon) and carry a pyrrole group and a phenyl hydroxyl group that are both ionizable groups. Analysis of pyrrolomycins I and J suggests that the phenyl hydroxyl group of pyrrolomycins C and D plays an important role in this proton gradient uncoupling. Predictions of the acid dissociation constant (pK_a, 5.1; Fig. S4) of the hydroxyl group of pyrrolomycins suggests that it would allow the shuttling of protons from outside to inside the bacteria and thus uncouple the proton motive force (as depicted in Fig. 6). The lipophilic nature of the pyrrolomycins likely favors their localization in the nonpolar membrane lipids, cycling from the outer leaflet to the inner leaflet to shuttle protons. To support this, the chlorine-rich FabI inhibitor triclosan has also been shown to act as a protonophore using its phenyl hydroxyl group to shuttle protons across the membrane (26). In line with these findings, the cytotoxicity observed with pyrrolomycins is likely due to the observed protonophore activity on mitochondrial membranes.

A number of natural products have been described to exhibit protonophoric activity, including usnic acid (27), hypericin (28), clusianone (29), polyphenols (30), and others. Nonetheless, all these molecules are less potent than the conventional proton uncoupler CCCP. This work demonstrates that pyrrolomycins C and D are an order of magnitude more active than CCCP and, to our knowledge, the most potent known protonophores. It is plausible that natural products such as pyoluteorin, TAN-876B, and marinopyrroles, which have strong structural similarities to pyrrolomycins, may also act as protonophores.

This work illustrates the importance of evaluating the mechanism of action of antibiotic molecules before developing them as potential drugs. We show that pyrrolomycins are potent inhibitors of bacterial membrane potential through their protonophore activity that allows for the specific shuttling of protons across polarized lipid membrane bilayers. This potent activity, which is an order of magnitude higher than that of the benchmark CCCP, explains its broad spectrum of antibiotic activity and provides an explanation for their acute cytotoxic effects found *in vitro* and reported *in vivo*.

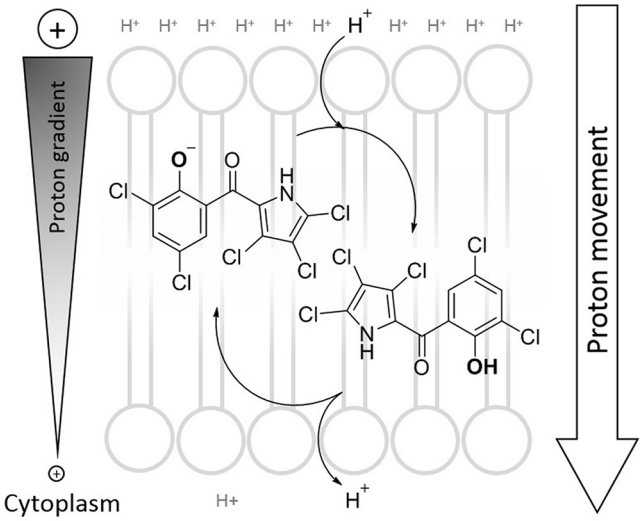

FIG 6 Model of the proton gradient uncoupling by pyrrolomycins. Lipophilic pyrrolomycins likely accumulate in the nonpolar lipid membrane because of their physical chemical properties. When oriented to the less acidic internal side of the cytoplasmic membrane leaflet, the pyrrolomycin hydroxyl group will preferentially ionize, releasing a proton into the cytoplasm. When flipped to the outer leaflet of the membrane, the more acidic environment will favor the protonation of the hydroxyl group and, hence, the uptake of an extracytoplasmic proton, which in turn will be released in the cytosol. Overall, the cycling of this process will allow for the net movement of protons from outside the bacterial cell to the inside, uncoupling of the proton gradient, and disturbance of the membrane proton motive force.

MATERIALS AND METHODS

Strains and media. *Staphylococcus aureus* SH1000 was kindly provided by S. J. Foster (University of Sheffield). *Escherichia coli* BW25113 (CGSC 7636) and its derivatives *E. coli* Δ*tolC* (JW5503-1, Δ*tolC732*::*kan*, CGSC 11430), *E. coli* Δ*acrA* (JW0452-3, Δ*acrA748*::*kan*, CGSC 11843), and *E. coli* Δ*acrB* (JW0451-2, Δ*acrB747*::*kan*, CGSC 8609) were obtained from the Coli Genetic Stock Center (CGSC) and originated from the Keio Collection (31). *Mycobacterium tuberculosis* H37Rv was kindly provided by the Institut Pasteur in Paris, France. *Acinetobacter baumannii* LMG1025, *Pseudomonas aeruginosa* LMG 12228, *Klebsiella pneumoniae* LMG 2095, and *Streptococcus pneumoniae* LMG 14545 were obtained from the BCCM/LMG bacterial collection. HepG2 (HB-8065) and HEK-293T (CRL-3216TM) cell lines originated from the American Type Culture Collection (ATCC).

M. tuberculosis was conventionally grown in Middlebrook 7H9 supplemented with 10% OADC, 0.2% glycerol, and 0.05% Tween 80 or, to evaluate the impact of bovine serum albumin (BSA), in Middlebrook 7H9 supplemented with 0.2% glucose, 0.2% glycerol, 0.01% tyloxapol, 0.095% NaCl, and with or without 0.5% BSA. All other bacteria were grown in cation-adjusted Mueller-Hinton broth (CAMHB; Difco), alone or with supplementation of 10% fetal calf serum (FCS) or 0.5% BSA. Both HepG2 and HEK-293 cells were cultured and tested in Dulbecco's modified Eagle medium (DMEM) supplemented with 10% FCS.

Chemical synthesis of pyrrolomycins C, D, I, and J. Pyrrolomycins C, D, I, and J were chemically synthesized as described previously (8, 32, 33) and are summarized in the supplemental material. The chemical identity and structures were confirmed by high-resolution mass spectrometry and ^{1}H-NMR in comparison to literature data.

Determination of MIC, MBC, and cytotoxicity. The MICs for *E. coli*, *S. aureus*, *S. pneumoniae*, *M. tuberculosis*, *A. baumannii*, and *K. pneumoniae* were determined using the colorimetric resazurin microtiter assay (REMA). Briefly, compounds dissolved in dimethyl sulfoxide (DMSO) were distributed by an Echo liquid handler (Labcyte) into the wells of a 384-well plate (500 nl of compound/DMSO per well). Plates were subsequently incubated with a diluted bacterial culture (50 μl) and incubated (see Table S1 for conditions). Bacterial viability was then determined by the resazurin reduction assay, as measured by fluorescence (excitation [Ex], 530 nm; emission [Em], 590 nm). For *P. aeruginosa*, which does not allow the entry of resazurin, bacterial viability was determined by the bacterial optical density at 600 nm (OD_{600}). For all experiments, rifampin or ciprofloxacin was run in parallel as a control.

Solid MICs were determined by mixing autoclaved CAMHB with 1.5% agar with compound dilutions in DMSO in a 96-well plate. Bacteria were then added to the solidified medium (5 μl OD of 0.001), and wells were scored for growth after 24 and 48 h of incubation (37°C).

The minimal bactericidal concentration (MBC) was determined by measuring the impact of compounds on the CFU. Briefly, in a 96-well plate, 100 μl of bacterial suspension was incubated in the presence of compound. The number of viable bacteria was then determined at different time points by plating bacterial dilutions on LB agar, and the CFU were determined following overnight incubation at 37°C.

Cytotoxicity of pyrrolomycins. For cytotoxicity assays, compounds were added in DMSO to a 384-well plate by Echo liquid handling. Fifty microliters of HepG2 or HEK-293 cells in DMEM (without

phenol red) supplemented with 10% FCS was then seeded into each well (5,000 cells per well). Cells were incubated for 3 days (37°C, 5% CO_2), cellular viability was determined by the addition of resazurin (final concentration, 0.025%, 4 h), and fluorescence was determined (Ex, 530 nm; Em, 590 nm).

Isolation of pyrrolomycin D-resistant mutants, whole-genome sequencing, and variant analysis. The selection of *E. coli* or *S. aureus* pyrrolomycin D-resistant clones was performed by plating 100 μl of a concentrated log-phase culture (concentrated to OD_{600} of 1, 10, 100, and 500) onto CAMHB agar containing various concentrations of pyrrolomycin D. Plates were incubated for 48 h at 37°C to allow for the appearance of resistant colonies. Resistance of isolates was confirmed by growing colonies on CAMHB agar without pyrrolomycin D, followed by MIC analysis. Whole-genome sequencing and variant analysis of the resistant isolates and the parental wild-type were performed by Genoscreen (Lille, France). Identified genetic variations were confirmed by Sanger sequencing.

***E. coli* mutant construction.** To validate that the identified *alsR-mdtN* deletion in the *E. coli* Δ*tolC* mutant is the cause of resistance to pyrrolomycin D, this deletion was generated in the parental strain. For this, a number of strains were designed and are summarized in Fig. 2 and Table 2. The primers used are listed in Table S2.

To generate EP664, the BW25113 Δ*tolC*::Km Keio collection strain was transformed with pFLP2 encoding the FLP recombinase (34) to remove the kanamycin (Km) cassette. Ampicillin-resistant (Amp^r) transformants were screened for Km sensitivity (Km^s) to assess excision of the FRT-Km-FRT cassette (Table S2). One such Amp^r Km^s mutant was further streaked on an LB–5% sucrose plate to cure pFLP2 and yield the unmarked Δ*tolC* derivative, EP664.

EP673 was constructed from EP664(pEP1436) by red recombination at 30°C (35) using the PCR product generated with primers RH296 and RH297 and the pEP1446 template (Table S2). Correct integration of the Km1446 cassette into the *als* locus was assessed by PCR with primers RH278 and RH279, and pEP1436 was cured by streaking on an LB–5% sucrose plate at 37°C.

To construct EP676, arabinose-induced EP673(pEP1436) was electrotransformed with the hybridized 78-mer oligonucleotides RH298 and RH299 (Table S2). Clones were selected at 30°C on LB-Amp plates containing doxycycline (100 μg/ml) and then screened for Km sensitivity. Correct allelic exchange was confirmed by PCR with primers RH278 and RH279 and by sequencing of the product. A Km^s clone was then cured of pEP1436 by streaking on an LB–5% sucrose plate at 37°C.

To obtain EP680, arabinose-induced EP676(pEP1436) was electrotransformed with the PCR product generated with primers RH300 and RH301 on the pEP1446 template (Table S2). Integration of the Km1446 cassette at the *mdtOP* locus was checked by PCR with primers RH279 and K2F. A Km^r clone was then cured of pEP1436 by streaking on an LB–5% sucrose plate at 37°C.

To construct EP705 (Δ*ompA* mutant) and EP706 (Δ*slyA* mutant), arabinose-induced EP664(pEP1436) was electrotransformed with the PCR product generated with primers RH732 and RH733, or RH728 and RH729 (Table S2) on the pEP1446 template. Integration of the Km1446 cassette in the *ompA* or *slyA* gene was checked by PCR with primer pairs RH734 and RH735 or RH730 and RH731, respectively. For each construct, a Km^r clone was then cured of pEP1436 by streaking on an LB–5% sucrose plate at 37°C.

Plasmid construction. To generate pEP714, *mdtP* was first PCR amplified from the BW25113 genome with the RH723-RH724 primer pair and cloned into pCRbluntIITopo. The absence of mutation in the insert was assessed by sequencing. Then, *mdtP* was subcloned into pBAD30 as a SalI-HindIII DNA fragment.

To construct pEP712, *alsR* was first PCR amplified from the BW25113 genome with the RH726-RH727 primer pair and cloned into pCRbluntIITopo. The absence of mutation in the insert was assessed by sequencing. Then, *alsR* was subcloned as a SalI-XbaI DNA fragment into pFU95 digested with the same enzymes to yield pEP712, in which *alsR* is transcribed from the strong constitutive promoter PgapA. The control empty plasmid pEP713 corresponds to the intramolecular ligation of digested pFU95.

Sample preparation for electron microscopy. Log-phase *E. coli* Δ*tolC* mutant and *S. aureus* SH1000 cultures grown in CAMHB were diluted to an OD_{600} of 0.4, and 400 μl of culture was placed in a well of a 24-well plate containing a sterile glass coverslip. Cells were incubated for 5 h at 37°C with or without 100 ng/ml pyrrolomycin D. After incubation, 400 μl of 2.5% (wt/vol) glutaraldehyde (in phosphate-buffered saline [PBS]) was added to the wells for 3 min. All of the supernatant was subsequently aspirated and the cells covered with 400 μl of 2.5% (wt/vol) glutaraldehyde (overnight, 4°C). Bacteria were fixed by the addition of glutaraldehyde (2.5% [wt/vol]) glutaraldehyde in PBS at 4°C overnight.

Scanning electron microscopy. After washing, the bacteria on the glass cover slide were treated with 1% osmium tetroxide in water (30 min in the dark). Bacteria were then dehydrated with increasing ethanol concentration baths up to 100% ethanol and dried with a critical point drier (Quorum Technologies K850, Elexience, France). The dry coverslips were then mounted on stubs and coated with 5 nm platinum (Quorum Technologies Q150T). Bacteria were observed by scanning electron microscopy using a secondary electron detector in a Merlin compact VP SEM (Zeiss, France) operated at 2 to 3 kV.

Membrane depolarization assay using $DiSC_3(5)$. Experiments using 3,3-dipropylthiacarbocyanine iodide $DiSC_3(5)$ were conducted under conditions similar to those described previously (18). Briefly, log-phase bacteria were pelleted (12,000 × *g*, 5 min) and washed twice in buffer A (10 mM potassium phosphate buffer [pH 7] containing 250 mM sucrose) for *S. aureus* and in buffer B (5 mM potassium phosphate [pH 7.3] and 20 mM glucose) for the *E. coli* Δ*tolC* mutant. Bacteria were then resuspended (to an OD_{600} of 0.085 for *S. aureus* and OD_{600} of 0.4 for the *E. coli* Δ*tolC* mutant) in their respective buffers with 10 μM $DiSC_3(5)$ and 100 mM KCl. One hundred microliters of cells was added to the wells of a 96-well plate and placed into a prewarmed (37°C) fluorescence plate reader (EnVision; Perkin Elmer). Bacterial accumulation of $DiSC_3(5)$ was followed by measuring $DiSC_3(5)$ fluorescence (excitation, 620 nm; emission, 685 nm) until it stabilized [fluorescence decreased due to fluorescence quenching upon $DiSC_3(5)$ accumulation in the bacteria]. Upon fluorescence stabilization, different concentrations of

pyrrolomycin or CCCP were added to the bacteria, and depolarization was followed by kinetic analysis of $DiSC_3(5)$ fluorescence. Experiments were also performed in the absence of bacteria to determine quenching of $DiSC_3(5)$ fluorescence by the compounds themselves. Bacterial membrane depolarization was determined as the compound-mediated increase in $DiSC_3(5)$ fluorescence 10 min postexposure.

Membrane depolarization assay using $DiOC_2(3)$. To follow bacterial membrane depolarization by 3,3′-dihexyloxacarbocyanine iodide [$DiOC_2(3)$], *S. aureus* was grown in CAMHB to a log-phase culture (OD_{600}, ~0.4). Bacteria were diluted 1:1,000 in PBS and 1 ml added to microtubes containing 10 μl of test compounds in DMSO at a 100× final concentration. Following a 15-min incubation at room temperature, 10 μl of 3 mM $DiOC_2(3)$ in DMSO was added to the bacteria, mixed, and incubated for a further 15 min. The bacteria were subsequently analyzed by flow cytometry using a AttuneNxT cytometer (Thermo Fisher). For flow cytometry parameters, initially, the bacterial population was selected on forward scatter/side scatter (FSC/SSC) dot plot read in logarithmic scale, using PBS as a control for background noise. Optimal parameters of threshold were found to be FSC 2 × 1,000 and SSC 0.1 × 1,000. $DiOC_2(3)$ fluorescence of the bacterial population was then analyzed in both the BL1 channel (excitation, 488 nm; emission, 530 nm) and BL2 channel (excitation, 488 nm; emission, 590 nm) for green and red fluorescence, respectively. Depolarization could be visualized as a decrease in BL1 fluorescence and an increase in BL2 fluorescence and was calculated using the BL2/BL1 ratio.

Liver mitochondrial respiration assay. Rat liver mitochondria were isolated by differential centrifugation (28) in a medium containing 250 mM sucrose, 5 mM MOPS, and 1 mM EGTA (pH 7.4). The final wash was performed in the medium additionally containing bovine serum albumin (0.1 mg/ml). The protein concentration was determined using the Biuret method. Handling of animals and experimental procedures were conducted in accordance with the international guidelines for animal care and use and were approved by the institutional ethics committee of the A. N. Belozersky Institute of Physico-Chemical Biology at Moscow State University.

Respiration of isolated mitochondria was measured using a standard polarographic technique with a Clark-type oxygen electrode (Strathkelvin Instruments, UK) at 25°C using the 782 system software. The incubation medium contained 250 mM sucrose, 5 mM MOPS, and 1 mM EGTA (pH 7.4). The mitochondrial protein concentration was 0.8 mg/ml. Oxygen uptake is expressed as nmol/min·mg protein.

BLM experiments to define the protonophore activity of pyrrolomycins. A bilayer lipid membrane (BLM) was formed by the brush (36) from a 2% decane solution of diphytanoylphosphatidylcholine (DPhPC) on a 0.6-mm aperture in a Teflon septum separating the experimental chamber into two compartments of equal 3-ml volumes. Electrical current across the BLM was measured under voltage-clamp conditions with two AgCl electrodes placed into the solutions on the two sides of the BLM via agar bridges, using a Keithley 428 amplifier (Cleveland, OH, USA). The voltage applied to the BLM was 50 mV.

SUPPLEMENTAL MATERIAL

Supplemental material for this article may be found at https://doi.org/10.1128/AAC.01450-19.

SUPPLEMENTAL FILE 1, PDF file, 1 MB.

ACKNOWLEDGMENTS

This work was funded by the ATIP Avenir young investigator program (CNRS/INSERM). We are thankful for the use of the NMR facility of the Institut Pasteur de Lille, a facility cofunded by the European Union with the European Regional Development Fund (ERDF), by the Hauts-de-France Regional Council (contract no. 17003781), Métropole Européenne de Lille (contract no. 2016_ESR_05), and French State (contract no. 2017-R3-CTRL-Phase 1). We thank Nicolas Barois (CIIL) and the BioImaging Center Lille for access to the SEM, equipment supported by the ANR (10-EQPX-04-01) and the EU-FEDER (12,001,407). We thank Alexandre Vandeputte and the HCS facility "Ariadne" that was supported by ANR and by the Feder (ANR-10-EQPX-04-01/Equipex Imaginex BioMed). We thank the Flow Core Facility–BioImaging Center Lille for access to AttuneNxT cytometry.

REFERENCES

1. O'Neill J. 2014. Antimicrobial resistance: tackling a crisis for the health and wealth of nations. The review on antimicrobial resistance. Review on Antimicrobial Resistance, London, United Kingdom. https://amr-review.org/sites/default/files/AMR%20Review%20Paper%20-%20Tackling%20a%20crisis%20for%20the%20health%20and%20wealth%20of%20nations_1.pdf.
2. Newman DJ, Cragg GM. 2016. Natural products as sources of new drugs from 1981 to 2014. J Nat Prod 79:629–661. https://doi.org/10.1021/acs.jnatprod.5b01055.
3. Ezaki N, Koyama M, Shomura T, Tsuruoka T, Inouye S. 1983. Pyrrolomycins C, D and E, new members of pyrrolomycins. J Antibiot 36:1263–1267. https://doi.org/10.7164/antibiotics.36.1263.
4. Zhang X, Parry RJ. 2007. Cloning and characterization of the pyrrolomycin biosynthetic gene clusters from Actinosporangium vitaminophilum ATCC 31673 and Streptomyces sp. strain UC 11065. Antimicrob Agents Chemother 51:946–957. https://doi.org/10.1128/AAC.01214-06.
5. Charan RD, Schlingmann G, Bernan VS, Feng X, Carter GT. 2005. Additional pyrrolomycins from cultures of streptomyces fumanus. J Nat Prod 68:277–279. https://doi.org/10.1021/np0496542.
6. Schillaci D, Petruso S, Raimondi MV, Cusimano MG, Cascioferro S, Scalisi

M, La Giglia MA, Vitale M. 2010. Pyrrolomycins as potential antistaphylococcal biofilms agents. Biofouling 26:433–438. https://doi.org/10.1080/08927011003718673.
7. Schillaci D, Petruso S, Cascioferro S, Raimondi MV, Haagensen JAJ, Molin S. 2008. In vitro anti-Gram-positive and antistaphylococcal biofilm activity of newly halogenated pyrroles related to pyrrolomycins. Int J Antimicrob Agents 31:380–382. https://doi.org/10.1016/j.ijantimicag.2007.10.013.
8. Yang Z, Liu Y, Ahn J, Qiao Z, Endres JL, Gautam N, Huang Y, Li J, Zheng J, Alnouti Y, Bayles KW, Li R. 2016. Novel fluorinated pyrrolomycins as potent anti-staphylococcal biofilm agents: Design, synthesis, pharmacokinetics and antibacterial activities. Eur J Med Chem 124:129–137. https://doi.org/10.1016/j.ejmech.2016.08.017.
9. Wayne LG. 1994. Cultivation of Mycobacterium tuberculosis for research purposes, p 73–83. *In* Bloom BR (ed), Tuberculosis: pathogenesis, protection, and control. American Society of Microbiology, Washington, DC.
10. Curran TD, Abacha F, Hibberd SP, Rolfe MD, Lacey MM, Green J. 2017. Identification of new members of the Escherichia coli K-12 MG1655 SlyA regulon. Microbiology 163:400–409. https://doi.org/10.1099/mic.0.000423.
11. Navarre WW, Halsey TA, Walthers D, Frye J, McClelland M, Potter JL, Kenney LJ, Gunn JS, Fang FC, Libby SJ. 2005. Co-regulation of Salmonella enterica genes required for virulence and resistance to antimicrobial peptides by SlyA and PhoP/PhoQ. Mol Microbiol 56:492–508. https://doi.org/10.1111/j.1365-2958.2005.04553.x.
12. Choi U, Lee C-R. 2019. Distinct roles of outer membrane porins in antibiotic resistance and membrane integrity in Escherichia coli. Front Microbiol 10:953. https://doi.org/10.3389/fmicb.2019.00953.
13. Yang SJ, Xiong YQ, Dunman PM, Schrenzel J, François P, Peschel A, Bayer AS. 2009. Regulation of mprF in daptomycin-nonsusceptible Staphylococcus aureus strains. Antimicrob Agents Chemother 53:2636–2637. https://doi.org/10.1128/AAC.01415-08.
14. Ernst CM, Peschel A. 2011. Broad-spectrum antimicrobial peptide resistance by MprF-mediated aminoacylation and flipping of phospholipids. Mol Microbiol 80:290–299. https://doi.org/10.1111/j.1365-2958.2011.07576.x.
15. Komatsuzawa H, Ohta K, Fujiwara T, Choi GH, Labischinski H, Sugai M. 2001. Cloning and sequencing of the gene, *fmtC*, which affects oxacillin resistance in methicillin-resistant *Staphylococcus aureus*. FEMS Microbiol Lett 203:49–54. https://doi.org/10.1111/j.1574-6968.2001.tb10819.x.
16. Peschel A, Jack RW, Otto M, Collins LV, Staubitz P, Nicholson G, Kalbacher H, Nieuwenhuizen WF, Jung G, Tarkowski A, van Kessel KPM, van Strijp J. 2001. *Staphylococcus aureus* resistance to human defensins and evasion of neutrophil killing via the novel virulence factor Mprf is based on modification of membrane lipids with L-lysine. J Exp Med 193:1067–1076. https://doi.org/10.1084/jem.193.9.1067.
17. Chileveru HR, Lim SA, Chairatana P, Wommack AJ, Chiang I-L, Nolan EM. 2015. Visualizing attack of Escherichia coli by the antimicrobial peptide human defensin 5. Biochemistry 10:1767–1777. https://doi.org/10.1021/bi501483q.
18. Te Winkel JD, Gray DA, Seistrup KH, Hamoen LW, Strahl H. 2016. Analysis of antimicrobial-triggered membrane depolarization using voltage sensitive dyes. Front Cell Dev Biol 4:29. https://doi.org/10.3389/fcell.2016.00029.
19. Benz R. 1988. Structural requirement for the rapid movement of charged molecules across membranes. Experiments with tetraphenylborate analogues. Biophys J 54:25–33. https://doi.org/10.1016/S0006-3495(88)82927-8.
20. Rokitskaya TI, Kosenko ID, Sivaev IB, Antonenko YN, Bregadze VI. 2017. Fast flip-flop of halogenated cobalt bis(dicarbollide) anion in a lipid bilayer membrane. Phys Chem Chem Phys 19:25122–25128. https://doi.org/10.1039/C7CP04207H.
21. Takeda R. 1958. Structure of a new antibiotic, pyoluteorin. J Am Chem Soc 80:4749–4750. https://doi.org/10.1021/ja01550a093.
22. Funabashi Y, Takizawa M, Tsubotani S, Tanida S, Harada S, Kamiya K. 1992. Chemistry and biological activities of new pyrrole antibiotics, TAN-876 A and B. J Tak Res Lab 51:73–89.
23. Hughes CC, Kauffman CA, Jensen PR, Fenical W. 2010. Structures, reactivities, and antibiotic properties of the marinopyrroles A–F. J Org Chem 75:3240–3250. https://doi.org/10.1021/jo1002054.
24. Ling LL, Schneider T, Peoples AJ, Spoering AL, Engels I, Conlon BP, Mueller A, Schäberle TF, Hughes DE, Epstein S, Jones M, Lazarides L, Steadman VA, Cohen DR, Felix CR, Fetterman KA, Millett WP, Nitti AG, Zullo AM, Chen C, Lewis K. 2015. A new antibiotic kills pathogens without detectable resistance. Nature 517:455–459. https://doi.org/10.1038/nature14098.
25. Silverman JA, Oliver N, Andrew T, Li T. 2001. Resistance studies with daptomycin. Antimicrob Agents Chemother 45:1799–1802. https://doi.org/10.1128/AAC.45.6.1799-1802.2001.
26. Popova LB, Nosikova ES, Kotova EA, Tarasova EO, Nazarov PA, Khailova LS, Balezina OP, Antonenko YN. 2018. Protonophoric action of triclosan causes calcium efflux from mitochondria, plasma membrane depolarization and bursts of miniature end-plate potentials. Biochim Biophys Acta Biomembr 1860:1000–1007. https://doi.org/10.1016/j.bbamem.2018.01.008.
27. Antonenko YN, Khailova LS, Rokitskaya TI, Nosikova ES, Nazarov PA, Luzina OA, Salakhutdinov NF, Kotova EA. 2019. Mechanism of action of an old antibiotic revisited: Role of calcium ions in protonophoric activity of usnic acid. Biochim Biophys Acta Bioenerg 1860:310–316. https://doi.org/10.1016/j.bbabio.2019.01.005.
28. Sell TS, Belkacemi T, Flockerzi V, Beck A. 2014. Protonophore properties of hyperforin are essential for its pharmacological activity. Sci Rep 4:7500. https://doi.org/10.1038/srep07500.
29. Reis FHZ, Pardo-Andreu GL, Nuñez-Figueredo Y, Cuesta-Rubio O, Marín-Prida J, Uyemura SA, Curti C, Alberici LC. 2014. Clusianone, a naturally occurring nemorosone regioisomer, uncouples rat liver mitochondria and induces HepG2 cell death. Chem Biol Interact 212:20–29. https://doi.org/10.1016/j.cbi.2014.01.015.
30. Zholobenko AV, Mouithys-Mickalad A, Dostal Z, Serteyn D, Modriansky M. 2017. On the causes and consequences of the uncoupler-like effects of quercetin and dehydrosilybin in H9c2 cells. PLoS One 12:e0185691. https://doi.org/10.1371/journal.pone.0185691.
31. Baba T, Ara T, Hasegawa M, Takai Y, Okumura Y, Baba M, Datsenko KA, Tomita M, Wanner BL, Mori H. 2006. Construction of Escherichia coli K-12 in-frame, single-gene knockout mutants: the Keio collection. Mol Syst Biol 2:2006.0008. https://doi.org/10.1038/msb4100050.
32. Koyama M, Ezaki N, Tsuruoka T, Inouye S. 1983. Structural studies on pyrrolomycins C, D and E. J Antibiot (Tokyo) 36:1483–1489. https://doi.org/10.7164/antibiotics.36.1483.
33. Martin R, Risacher C, Barthel A, Jäger A, Schmidt AW, Richter S, Böhl M, Preller M, Chinthalapudi K, Manstein DJ, Gutzeit HO, Knölker H-J. 2014. Silver(I)-catalyzed route to pyrroles: synthesis of halogenated pseudilins as allosteric inhibitors for myosin ATPase and X-ray crystal structures of the protein-inhibitor complexes. Eur J Org Chem 2014:4487–4505. https://doi.org/10.1002/ejoc.201402177.
34. Hoang TT, Karkhoff-Schweizer RR, Kutchma AJ, Schweizer HP. 1998. A broad-host-range F1p-FRT recombination system for site-specific excision of chromosomally-located DNA sequences: application for isolation of unmarked Pseudomonas aeruginosa mutants. Gene 212:77–86. https://doi.org/10.1016/s0378-1119(98)00130-9.
35. Datsenko KA, Wanner BL. 2000. One-step inactivation of chromosomal genes in Escherichia coli K-12 using PCR products. Proc Natl Acad Sci U S A 97:6640–6645. https://doi.org/10.1073/pnas.120163297.
36. Mueller P, Rudin DO, Tien HT, Wescott WC. 1963. Methods for the formation of single bimolecular lipid membranes in aqueous solutiuon. J Phys Chem 67:534–535. https://doi.org/10.1021/j100796a046.